

# Tissue Plasminogen Activator Expression Is Restricted to Subsets of Excitatory Pyramidal Glutamatergic Neurons

Morgane Louessard<sup>1</sup> · Alexandre Lacroix<sup>2,3,4</sup> · Magalie Martineau<sup>5</sup> ·  
Gregoire Mondielli<sup>6</sup> · Axel Montagne<sup>1</sup> · Flavie Lesept<sup>1</sup> · Bertrand Lambolez<sup>2,3,4</sup> ·  
Bruno Cauli<sup>2,3,4</sup> · Jean-Pierre Mothet<sup>6</sup> · Denis Vivien<sup>1</sup> · Eric Maubert<sup>1</sup>

Received: 4 June 2015 / Accepted: 7 September 2015 / Published online: 16 September 2015  
© Springer Science+Business Media New York 2015

**Abstract** Although the extracellular serine protease tissue plasminogen activator (tPA) is involved in pathophysiological processes such as learning and memory, anxiety, epilepsy, stroke, and Alzheimer's disease, information about its regional, cellular, and subcellular distribution in vivo is lacking. In the present study, we observed, in healthy mice and rats, the presence of tPA in endothelial cells, oligodendrocytes, mastocytes, and ependymocytes, but not in pericytes, microglial cells, and astrocytes. Moreover, blockage of the axo-dendritic transport unmasked tPA expression in neurons of cortical and hippocampal areas. Interestingly, combined electrophysiological recordings, single-cell reverse

transcription polymerase chain reaction (RT-PCR), and immunohistological analyses revealed that the presence of tPA is restricted to subsets of excitatory pyramidal glutamatergic neurons. We further evidenced that tPA is stored in synaptobrevin-2-positive glutamatergic synaptic vesicles. Based on all these data, we propose the existence of tPA-ergic neurons in the mature brain.

**Keywords** Extracellular protease · Neurotransmission · Cortical neurons · Tissue-type plasminogen activator

Denis Vivien and Eric Maubert contributed equally to this work.

**Electronic supplementary material** The online version of this article (doi:10.1007/s12035-015-9432-7) contains supplementary material, which is available to authorized users.

✉ Denis Vivien  
vivien@cyceron.fr

<sup>1</sup> INSERM, UMR-S 919, Serine Proteases and Pathophysiology of the Neurovascular Unit, Université Caen Basse-Normandie, GIP Cyceron, Bvd Henri Becquerel, GIP Cyceron, 14074 Caen, France

<sup>2</sup> UPMC Univ Paris 06, Institut de Biologie Paris-Seine (IBPS), UM 119, Neuroscience Paris Seine, Sorbonne Universités, 75005 Paris, France

<sup>3</sup> CNRS, UMR 8246, Neuroscience Paris Seine, 75005 Paris, France

<sup>4</sup> INSERM, UMR-S 1130, Neuroscience Paris Seine, 75005 Paris, France

<sup>5</sup> Department of Cellular Biophysics, Institute for Medical Physics and Biophysics, University of Muenster, Muenster, Germany

<sup>6</sup> Centre de Recherche en Neurobiologie et Neurophysiologie de Marseille UMR7286 CNRS, Aix Marseille University, Marseille, France

## Introduction

Due to its high affinity for fibrin and its ability to activate plasminogen into plasmin [1], tissue plasminogen activator (tPA) is a key protease of the fibrinolytic system [2]. In addition to its roles in the vascular system, tPA plays crucial functions in the central nervous system (CNS) acting either as an enzyme or a growth-factor-like molecule. Thus, tPA is involved in several physiological and pathological CNS processes, including learning and memory, anxiety, epilepsy, stroke, Alzheimer's disease, and spinal cord injury [3–9]. The neuronal functions of tPA are achieved through plasminogen-dependent or plasminogen-independent effects [10]. For instance, tPA-mediated generation of plasmin controls the degradation of the extracellular matrix [11], leading to axonal growth during development or neuronal death during brain injuries. In addition, tPA can process pro-neurotrophins including the pro-nerve growth factor (pro-NGF) or the pro-brain-derived neurotrophic factor (pro-BDNF) into their mature forms [12, 13]. tPA is also known to bind and/or activate a set of receptors such as low-density lipoprotein receptor-related proteins (LRPs) [14–16], N-methyl-D-aspartate receptor (NMDAR) [17, 18], annexin-II

[19], and epidermal growth factor receptors (EGFRs) [20]. All this information strikingly contrasts with our ignorance of the regional, cellular, and subcellular distribution of tPA in the CNS.

In the present study, we first characterized the cellular distribution of tPA in the healthy brain. Blockage of the axodendritic transport allowed us to unmask tPA-positive cortical neurons. Combining electrophysiological recordings with single-cell reverse transcription polymerase chain reaction (RT-PCR) and using histological and biochemical analyses, we revealed that tPA-positive neurons are a subpopulation of excitatory pyramidal glutamatergic neurons with tPA stored in synaptobrevin-2-positive glutamatergic synaptic vesicles. Altogether, this study highlights the existence of a subpopulation of excitatory tPA-ergic neurons.

## Materials and Methods

### Animals

Male Swiss mice ( $n=6$ ), tPA deficient (tPA knockout (KO);  $n=4$ ), their C57Bl6/J wild-type control ( $n=4$ ), and Wistar rats ( $n=6$ ; 8–10 weeks) were provided by CURB (Caen, France). Young Wistar rats ( $n=16$ ; postnatal days 15–21; Janvier) were used for patch-clamp recordings. Animals were housed with a 12-h light/12-h dark cycle in standard polypropylene cages (Charles River, France) with free access to water and food (SDS Dietex, France). Experiments were performed in accordance with the French (Decree 87/848) and the European Communities Council (Directive 86/609) guidelines.

### Immunohistochemistry

Control or treated mice and rats were deeply anesthetized and transcardially perfused with 0.9 % NaCl heparinized followed by a mixture of 2 % paraformaldehyde and 0.2 % picric acid in 0.1 M sodium phosphate buffer, pH 7.4 (150 or 400 ml, respectively). Brains were removed, washed in veronal buffer containing 20 % sucrose, and frozen in Tissue-Tek (Miles Scientific). Coronal sections (8–10  $\mu\text{m}$ ) were cut on a cryostat, collected on poly-D-lysine slides, and stored at  $-80^\circ\text{C}$ .

Coronal adjacent brain sections were incubated, overnight at room temperature, with primary antisera alone or in double-labeling experiments. Adapted secondary F(ab')<sub>2</sub> coupled to TRITC or fluorescein isothiocyanate (FITC; 1:600; Jackson ImmunoResearch, West Grove, USA) was used for visualization under epifluorescence or confocal microscopy illumination. Washed sections were coverslipped with antifade medium containing DAPI. Sections were examined with a microscope (DM6000; Leica). Images were digitally captured using a camera (CoolSNAP; Photometrics) and/or with an inverted confocal microscope (SP5, Leica). Images were visualized

respectively with Metavue 5.0 software (Molecular Devices, USA) and LAS AF lite software (LEICA). All the studies of immunohistochemistry raised against tPA presented in this manuscript were performed with a rabbit anti-tPA (generous gift from R. Lijnen, Leuven). tPA immunoserum was pre-incubated overnight with rtPA which resulted in the abolition of labeling in both mouse and rat blood vessels as in mice mossy fiber pathway. The specificity of tPA immunostainings was undoubtedly reinforced by the fact that a sheep commercial antibody gives similar immunostainings in both mouse and rat sections. Pilot experiments were performed to confirm the specificity and the optimal dilution of the various primary commercial antisera used. In all single-labeling experiments, F(ab')<sub>2</sub> fragments gave no labeling in any immunoreaction where the respective primary antiserum was omitted. Single labeling was carried out in parallel with double labeling on adjacent sections, and we ensured that each primary antibody gave similar results in single- or double-staining experiments. The detection of mastocytes was performed with Avidin fluorescein at 1/800 (A2901 Sigma). See all antibodies used in the Supplementary Table S1.

### In Vivo Colchicine Treatment

Mice and rats were deeply anesthetized and maintained with 2 % isoflurane in a 70 %/30 % gas mixture (N<sub>2</sub>O/O<sub>2</sub>) and the rectal temperature was maintained at  $37\pm 0.5^\circ\text{C}$ . Anesthetized mice and rats were placed into Kopf stereotaxic instrument. The skulls were exposed and small bore holes were drilled with a dental burr to allow intraventricular injection to be targeted by borosilicate glass pipettes (mice anteroposterior (AP)  $-0.2$  mm from bregma, lateral (L)  $\pm 1$  mm from midline, and ventral (V)  $-2.0$  mm deep to the surface; and rats AP  $-0.92$  mm from bregma, L  $\pm 1.5$  mm from midline, and V  $-3.4$  mm deep to the surface). Half of animals in each group were injected with 35 or 150  $\mu\text{g}$  of colchicine in solution (Sigma-Aldrich) for mice and rats, respectively, and the other half were injected with the vehicles. The dose of colchicine injected was chosen based on previous work [21, 22].

### Quantification of Cortical tPA-Positive Neurons

The image analysis was performed using ImageJ software. The proportion of neurons expressing tPA was obtained by dividing the total number of neurons (as revealed by Fox3 immunostaining) by the number of tPA-positive neurons in the retrosplenial granular cortex, the primary somatosensory cortex, the perirhinal cortex, and the piriform cortex. For each cortical area, three sections per animal were analyzed (5–9 images per cortical area per section ( $n=3$ ) per animal ( $N=3$ )). Cortical area was located using stereotaxic atlas.

## Whole-Cell Recordings

Young rats were decapitated, their brains quickly removed, and coronal slices (300  $\mu\text{m}$  thick) containing the barrel cortex were cut using a vibratome [23]. Individual slices were transferred to a recording chamber and perfused (1–2 ml/min) with oxygenated artificial cerebrospinal fluid (aCSF) containing (in millimolars) 126 NaCl, 2.5 KCl, 1.25  $\text{NaH}_2\text{PO}_4$ , 2  $\text{CaCl}_2$ , 1  $\text{MgCl}_2$ , 26  $\text{NaHCO}_3$ , 10 glucose, and 15 sucrose at 20–25  $^\circ\text{C}$ . Patch pipettes (4–8  $\text{M}\Omega$ ) were filled with 8  $\mu\text{l}$  of autoclaved K-gluconate-based RT-PCR internal solution [24]. Neurons were visualized in the slice using infrared videomicroscopy with Dodt gradient contrast optics. Whole-cell electrophysiological properties were recorded in current clamp mode as described previously [23]. Membrane potential values were not corrected for liquid junction potential.

## Single-Cell RT-PCR

At the end of the recording, the cell cytoplasm was aspirated in the recording pipette and expelled into a test tube, and reverse transcription (RT) was performed [25]. The single-cell RT-PCR protocol was designed to probe simultaneously for the expression of tPA and the neuronal markers vGluT1, the two isoforms of GAD (GAD65 and GAD67), three calcium-binding proteins [calbindin D28k (CB), calretinin (CR), and parvalbumin (PV)], and four neuropeptides [neuropeptide Y (NPY), vasoactive intestinal polypeptide (VIP), somatostatin (SOM), and cholecystokinin (CCK)]. Two amplification steps were performed essentially as described [24], with 10  $\mu\text{l}$  of the RT reaction products using the primer pairs (see Supplementary Table S2).

## Morphological Analysis of IR-DGC images

Somatic features were measured from IR-DGC images of the recorded cells as previously described [23]. Briefly, the soma was manually delineated using Image-Pro Analyzer 7.0.0.951 software (Media Cybernetics). Then, the length of major and minor axes, the perimeter, and the area were extracted. The soma elongation was calculated as the ratio between major and minor axes. Roundness was calculated as

$$\frac{\text{perimeter}^2}{4\pi \times \text{area}}$$

A value close to 1 is indicative of round somata.

## Isolation of Synaptic Vesicles

Synaptic vesicles (SVs) were isolated from brain ( $n=3$ ) of 2-month-old C57BL/6j mice using a combination of subcellular fractionation and size exclusion chromatography as described

previously [26] with minor modifications. Brains were surgically collected and were homogenized with a glass/Teflon homogenizer (10 strokes, 900 rpm) in 3 ml of ice-cold buffer (4 mM 4-(2-hydroxyethyl)-1-piperazineethanesulfonic acid (HEPES)-NaOH, pH7.4, and 320 mM sucrose)/1 g of brain. All the following steps were performed at 4  $^\circ\text{C}$ . The homogenate was centrifuged at 1000g for 10 min, and the supernatant S1 containing SVs was centrifuged at 15,000g for 15 min, giving S2 and P2. P2 was resuspended in 1 ml of homogenization buffer, and then 9 ml of ice-cold ddH<sub>2</sub>O was added to induce an osmotic shock and release SVs. This 10-ml mix was transferred into a glass/Teflon homogenizer (3 strokes, 2000 rpm) and centrifuged at 17,000g for 15 min. The resulting supernatant LS1 was combined with S2 and was centrifuged at 48,000g for 25 min. The supernatant CS1 was transferred into a glass/Teflon homogenizer (3 strokes, 900 rpm), and 5 ml of CS1 was overlaid onto 5 ml of 10 mM HEPES-KOH, pH 7.4, and 700 mM sucrose before centrifugation at 133,000g for 1 h. Fractions (500  $\mu\text{l}$  each) were collected starting from the top of the sucrose cushion. In fine, 20 sucrose fractions and a pellet were submitted to dot blot assays for Sb2 as a SV marker. Sb2-positive sucrose fractions were pooled together and centrifuged at 300,000g for 2 h. The pellet containing the SVs was resuspended in 1.8 ml of chromatography running buffer (100 mM Tris-HCl, pH 7.6, 100 mM KCl) and loaded on top of the size exclusion column (Kontes Chromaflex 100/1) packed with 70 ml of Sephacryl Superfine S-1000 matrix (GE Healthcare). The chromatography was controlled by an FPLC system (Pharmacia-Biotech LKB) at 100  $\mu\text{l}/\text{min}$ . The optical density at 280 nm was recorded online and fractions of 1 ml were collected. Fractions were analyzed by dot blot assays for the presence of Sb2. The Sb2-positive fractions were pooled and concentrated by centrifugation at 300,000g for 2 h and then resuspended in appropriate buffer for further analysis and stored at  $-80^\circ\text{C}$  until use. Fractions were analyzed by western blot for various surface organelle markers or for glutamate uptake assay.

## Immunoisolation of SVs

Immunoisolation of SVs was performed as previously described [27]. Briefly, the rat cerebral cortex of a male Wistar rat (2 months) was homogenized with a glass/Teflon homogenizer (10 strokes, 2500 rpm) in homogenization buffer (4 mM HEPES-KOH, pH 7.4, 100 mM K<sub>2</sub>-tartrate, 2 mM  $\text{MgCl}_2$ ). The homogenate was centrifuged for 25 min at 35,000g. The resulting supernatant S1 was incubated for 1 h with anti-Sb2 or with a murine IgG used as a control and 1 h with magnetic beads coupled to protein G (Ademtech). The beads were washed three times with homogenization buffer, and they were resuspended in appropriate buffer for further analysis.

## Protein Electrophoresis and Western Blot Assays

Proteins were separated by 10 or 12 % sodium dodecyl sulfate (SDS)-PAGE. Samples (3 µg/lane as determined by Bradford assay) were heated for 10 min at 60 °C (except for V-ATPase and for Na<sup>+</sup>/K<sup>+</sup>-ATPase, 10 min, at room temperature) under reducing and denaturing conditions in the presence of 20 mM DTT and 2.5 % (w/v) SDS. Proteins were transferred onto 0.22-µm nitrocellulose membranes (100 V for 1 h at room temperature). Membranes were blocked with Tris-suffered saline and Tween 20 (TBST)-5 % milk (1 h at room temperature) and then incubated with primary antibody (overnight at 4 °C). Membranes were washed three times in TBST-5 % milk and then probed with horseradish peroxidase (HRP)-conjugated secondary antibody diluted in TBST-5 % milk (1 h at room temperature). Membranes were washed three times for 5 min in TBST and then three times for 5 min in TBS. Finally, they were visualized using ECL Prime (GE Healthcare) with the G:BOX apparatus (Syngene).

## Glutamate Uptake Assay

Glutamate uptake was assessed by acidification assay using acidine orange (AO) as previously described [27]. Fractions from size exclusion chromatography containing SVs (~5 µg of proteins as determined by Bradford assay) were diluted in 50 µl of 10 mM HEPES-KOH, pH 7.4, 4 mM KCl, 4 mM MgSO<sub>4</sub>, and 320 mM sucrose. The reaction was started by adding 10 mM MgATP in a stirred microcuvette containing 20 µM AO, equilibrated at 32 °C. The reaction was stopped after 15–20 min by adding 50 mM (NH<sub>4</sub>)<sub>2</sub>SO<sub>4</sub> to dissipate the proton gradient across the vesicular membrane and release AO from the vesicular lumen. Changes of fluorescence were analyzed using a Photon Technology International spectrofluorimeter (excitation, 490 nm; emission, 530 nm). The acidification kinetics were analyzed using Felix32 software (Photon Technology International) for acquisition of AO fluorescence. Traces were normalized to the fluorescence at *t*<sub>0</sub> and corrected for baseline shifts induced by volume changes associated with the additions.

## Results

**Expression of tPA in CNS Cells.** The presence of tPA in the different cell types of the CNS was investigated by immunohistochemistry on perfused brain tissues from adult mice and rats (Fig. 1 and Supplementary Table S3). Immunostainings from hippocampal sections confirmed the presence of tPA in the mossy fiber pathway (from the hile of the dentate gyrus to the cornus ammonis 2) in wild-type (Fig. 1a, k) but not in tPA knockout mice (tPA KO, Fig. 1b) used as controls (similar findings were obtained in the cortex and medial habenula;

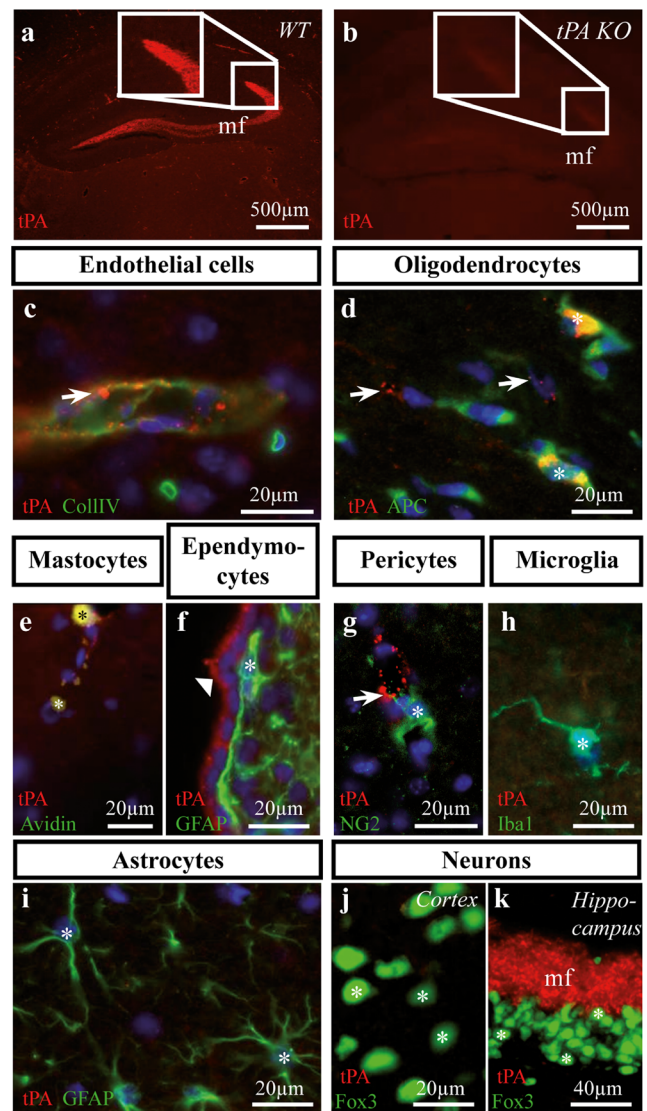


**Fig. 1** Cell type specificity of tPA expression in the adult mouse brain. **a, b** Specificity of tPA immunostainings (red). Whereas no immunoreactivity was detected in the mossy fiber (mf) of adult tPA knockout (tPA KO) mouse (**b**), positive immunostaining was revealed in adult wild-type (WT) mouse (**a**). **c–k** Localization of tPA immunoreactivity (tPA-ir) in CNS cells. Double immunofluorescent stainings performed with an antibody raised against tPA (red) in combination with a set of antibodies specific of each cell type analyzed (green). tPA-ir was observed in endothelial cells (**c, d, g**; arrows), the basal lamina was stained with an antibody raised against coll-IV (**c**), in some mature oligodendrocytes also positive for APC (**d**; stars), in mastocytes stained by avidin-FITC (**e**; stars), and ependymocytes underlying ventricles (**f**; arrowhead). tPA-ir was absent in NG2-positive pericytes (**g**; star), in Iba1-positive microglial cells (**h**; star), in GFAP-positive astrocytes (**f, i**; stars), and in the soma of Fox-3-positive cortical neurons (**j**; stars). tPA-ir was absent in the soma of Fox-3-positive hippocampal neurons (**k**). Positive immunostaining was revealed in the hippocampal mossy fiber (mf) (**k**). DAPI (blue) was used to reveal nuclei (**c–i**). (See also Supplementary Table S3) (Color figure online)

see Supplementary Fig. S1). tPA immunoreactivity was observed in endothelial cells (Fig. 1c, d, g, i), oligodendrocytes (Fig. 1d), mastocytes (Fig. 1e), and ependymocytes (Fig. 1f).

Pericytes (Fig. 1g), microglial cells (Fig. 1h), and astrocytes (Fig. 1f, i) were found negative for tPA immunostaining. No tPA-positive soma was revealed in cortical and hippocampal areas (Fig. 1j, k). Intriguingly, tPA immunostainings were restricted to nerve fibers in the hippocampus (mossy fibers; Fig. 1a), in the amygdala (Fig. 2a), the hypothalamic median eminence (Fig. 2b), the neurohypophysis (Fig. 2c), and the medial habenula (Fig. 2d).

**In Vivo Blockage of the Axo-dendritic Transport Unmasks tPA-Positive Neurons.** The lack of tPA immunoreactivity in cortical neurons was intriguing, considering the literature reporting a neuronal expression of tPA and subsequent functions [28–32]. We thus decided to block axo-dendritic transports by stereotaxic injections of colchicine in order to unmask the putative presence of tPA in neuronal cell bodies in the hippocampus (Supplementary Fig. S2) and in the cortex (Fig. 3). In the mouse hippocampus, colchicine treatment led to an accumulation of tPA in neuronal cell bodies of the dentate gyrus (Supplementary Fig. S2b vs S1b') associated with reduced levels of tPA in the corresponding mossy fibers that reached CA2 (Supplementary Fig. S2d vs S1d'). We also revealed an accumulation of tPA in pyramidal neuronal cell bodies in the different regions of the hippocampus: CA3, CA2, CA1 (Supplementary Fig. 2c–e vs S1c'–e') and in neuronal cell bodies of the fasciola cinereum (Supplementary Fig. 2f vs S1f'). Similarly, colchicine treatment unmasked the presence of tPA in cortical neurons and shrunken fibers (classically observed following treatment with colchicine) in both mice and rats (Fig. 3a, b vs 3a', b' and a'', b'' without vs after colchicine treatment, respectively).

Overall, we calculated that tPA-immunoreactive neurons accounted to around 15 % of the total number of neurons positive for Fox3 (4374 tPA-positive neurons of a total of 28,774 Fox3-positive neurons counted; Fig. 4d) in the retrosplinal granular cortex (Fig. 4c (a) and (b)), the primary somatosensory cortex (Fig. 4c (c) and (d)), the perirhinal cortex (Fig. 4c (e) and (f)), and the piriform cortex (Fig. 4c (g) and (h)). In some cortices, such as the somatosensory cortex (Fig. 4c (c)) or the perirhinal cortex (Fig. 4c (e)), tPA-immunoreactive neurons appeared more abundant in deeper layers, such as the layer V. Colchicine treatment did not affect the localization of tPA in the other cells of the CNS (Supplementary Fig. S3). tPA immunoreactivity was still observed in endothelial cells (Supplementary Fig. S3a, c, f, g), oligodendrocytes (Supplementary Fig. S3a), mastocytes (Supplementary Fig. S3b), ependymocytes (Supplementary Fig. S3c), and cortical neurons (Supplementary Fig. S3d). Microglial cells (Supplementary Fig. S3e), astrocytes (Supplementary Fig. S3f), and pericytes (Supplementary Fig. S3g) were still found negative for tPA.

**tPA-Positive Neurons Are Glutamatergic** We then investigated the neurochemical phenotype of the neurons containing tPA. The expression of neuronal tPA in layer V of the somatosensory cortex was studied by combining single-cell electrophysiological recordings and transcriptomic analyses (Fig. 5 and Supplementary Tables S4, S5, S6, S7, and S8). The single-cell RT-PCR protocol was designed for multiplex probing of the expression of tPA and 10 molecular markers classically used to define cortical neuronal subtypes [33]: the vesicular glutamate transporter 1 (vGluT1), the GABA-

**Fig. 2** Expression of tPA in fibers of the adult mouse brain. tPA-ir (red) was detected in fibers of the amygdala (a; arrows), in fibers of the hypothalamus median eminence (ME) (b; arrow), in fibers of the neurohypophysis (NH) (c; arrow) and in fibers of the medial habenula (d; arrow). DAPI (blue) was used to reveal nuclei (a–d) (Color figure online)

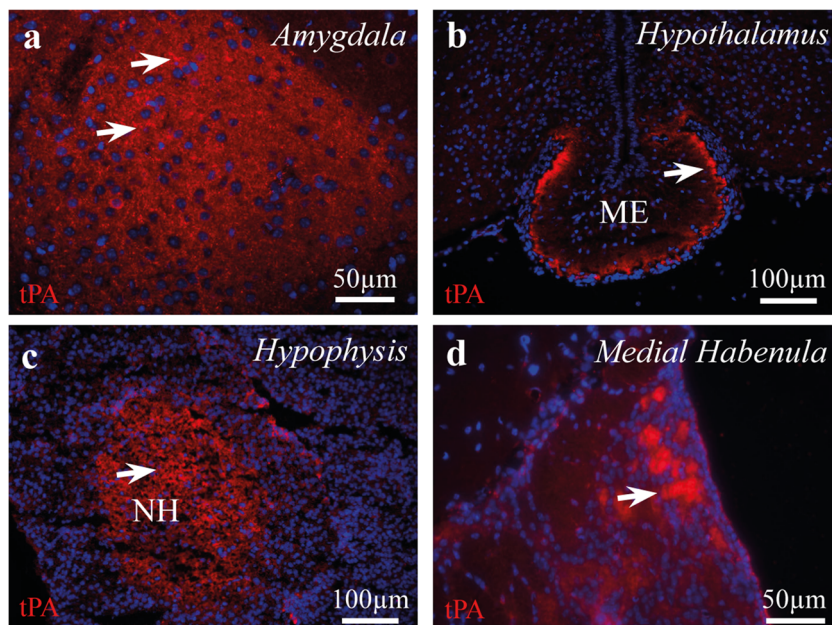
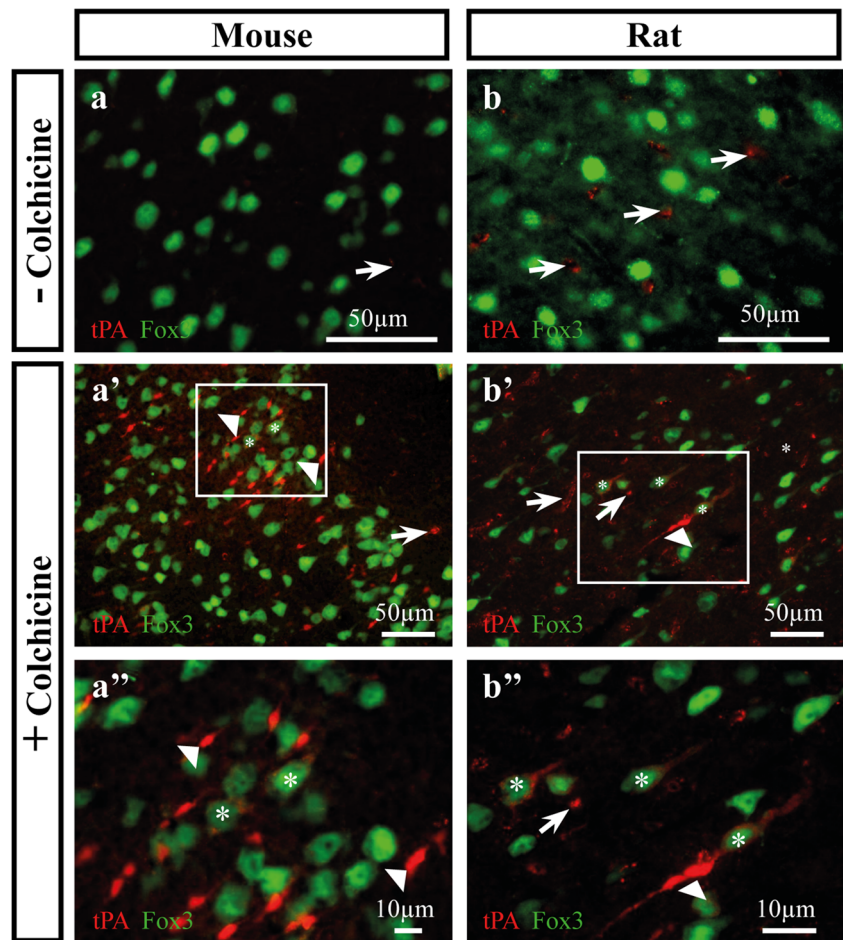


**Fig. 3** In vivo blockage of the axo-dendritic transport unmasks tPA-positive cortical neurons in both mouse and rat. Double immunofluorescent staining with the tPA antibody (red) and Fox3 antibody (green). No tPA-ir was detected in cortical neurons of untreated mice (a) and rats (b). In contrast, tPA-ir became positive in the soma of cortical neurons (stars) and in shrunken fibers (arrowheads; classically observed after colchicine treatment) from colchicine-treated mice (a' and a'') and rats (b' and b'') at low magnification (a', b') and high magnification (a'', b''). In both mice and rats, tPA-ir was seen in blood vessel walls (a, b, a', b', b''); arrow) (Color figure online)



synthesizing enzymes (glutamic acid decarboxylases, GAD 65 and GAD 67), three calcium-binding proteins (calretinin [CR], calbindin [CB], and parvalbumin [PV]), and four neuropeptides including vasoactive intestinal peptide (VIP), somatostatin (SOM), cholecystokinin (CCK), and neuropeptide Y (NPY). Pyramidal cells ( $n=30$ ) and interneurons ( $n=13$ ) were first selected according to their somatodendritic appearance and by their characteristic electrophysiological features [34, 35]. Detection of vGluT1 and absence of GAD (vGluT1+/GAD<sup>-</sup>) were indicative of a glutamatergic identity whereas detection of GAD (GAD<sup>+</sup>) denoted a GABAergic phenotype. The expression of tPA was observed in 3 cells out of 30 pyramidal neurons of the rat neocortical layer V (Fig. 5c) but was never detected in GABAergic interneurons ( $n=13$ ). The tPA-positive pyramidal cells expressed CCK in addition to vGluT1 (Fig. 5c). The electrophysiological signatures of the tPA-positive neurons did not significantly differ from the other pyramidal cells of the sample (Supplementary Tables S4, S5, S6, S7, and S8). Cortico-cortical layer V pyramidal cells exhibit significantly higher input resistance and smaller hyperpolarization-activated cationic current (sag; see Supplementary Table S4) than pyramidal cells projecting subcortical structures [36, 37]. Among the tPA-positive pyramidal

cells, some were putative subcortical neurons displaying relatively low input resistance (166 and 316 M $\Omega$ ) and large sag (28 and 36 %), and the others were presumably cortico-cortical (630 M $\Omega$  and 20 %). Accordingly, the tPA-positive subcortical pyramidal cells recovered for biocytin labeling exhibited a prominent apical dendrite with an extension in layer I (Fig. 5b) which is not observed in cortico-cortical pyramidal cells [36]. These results suggest that tPA-positive pyramidal cells are diverse and cannot be assigned to a specific subtype defined by a projection target [38, 39]. To confirm pyramidal identity of tPA-positive neurons at the population level, immunohistochemistry for vGluT1, GAD67, CCK, and T-box brain 1 (tbR1), a transcription factor characteristic of glutamatergic neurons [40], was performed from both mouse (Fig. 6a, c, e, g) and rat (Fig. 6b, d, f, h) brain tissues pre-treated with colchicine. We confirmed the presence of tPA in neurons also immunopositive for vGluT1 (Fig. 6a, b), CCK8 (Fig. 6c, d), or tbR1 (Fig. 6e, f) in cortical areas of both species. In contrast, tPA-positive neurons were negative for GAD67 (Fig. 6g, h). These data provide the first evidence that the cortical neurons that express tPA correspond to a subpopulation of glutamatergic pyramidal cells.

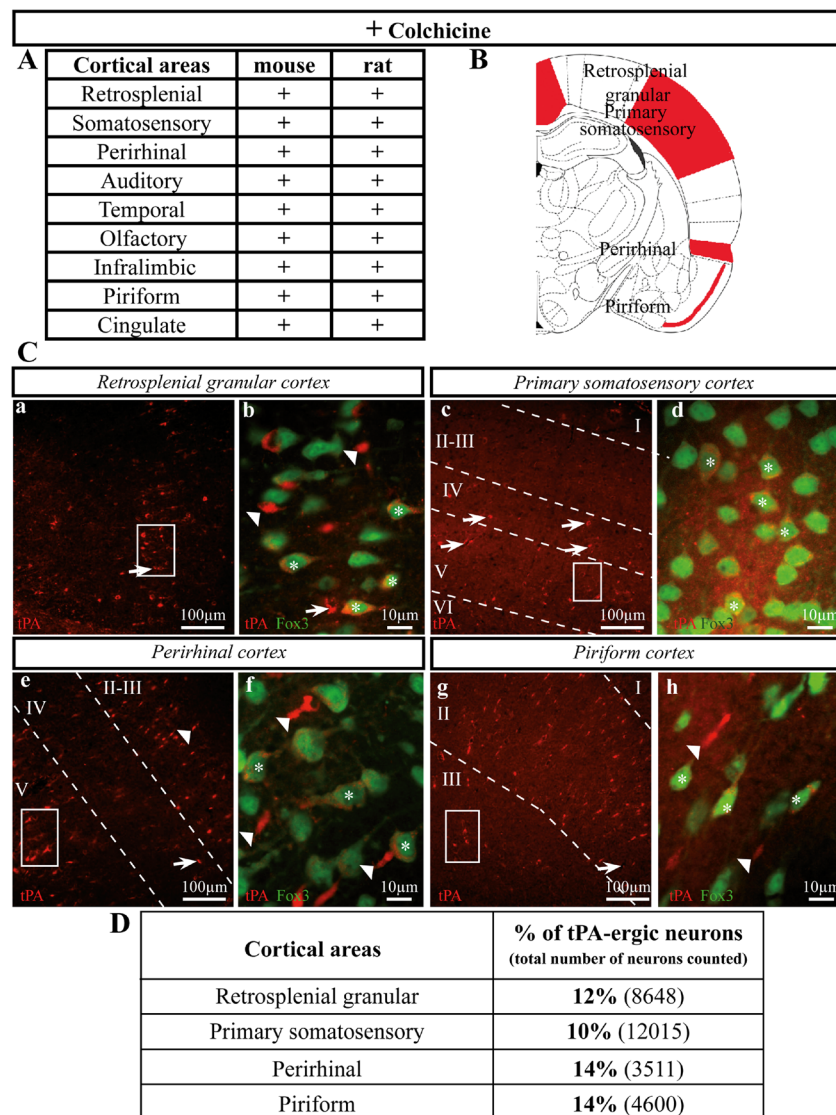


**Fig. 4** Distribution of tPA-positive neurons in cortical areas. **a** Immunohistochemistry performed on cortical sections from colchicine-treated mice and rats revealed tPA-positive neurons in all cortices. **b** Schematic representation of cortical areas in which we illustrated the distribution of tPA-positive neurons in **(c)**. **c** Illustration of some tPA-positive cortical neurons unmasked by colchicine treatment. Distribution of tPA-ir (red) was shown at low magnification (**a, c, e, g**) and corresponding *inserts* are seen at high magnification (**b, d, f, h**). In retrosplenial granular cortex, tPA-ir was observed in neurons of layers II–III (**a, b**; *stars*) and in shrunken fibers (**b**; *arrowheads*). In primary

somatosensory cortex, note the tPA-ir in layers II–III, V, and VI (**c, d**; *stars*). In perirhinal cortex, tPA-ir was seen in neurons of layer II–III (**e, f**; *stars*) and V (**e**) and in shrunken fibers (**e, f**; *arrowheads*). In piriform cortex, tPA-ir was observed in layers II–III (**g, h**; *stars*) and in shrunken fibers (**h**; *arrowheads*). Fox3 (green) was used to reveal neuronal cell bodies at higher magnification (**b, d, f, h**). tPA-ir was also observed in blood vessel walls (**a–c, e, g**; *arrows*). **d** Percentage of tPA-positive neurons in different cortical areas of colchicine-treated adult rats (Color figure online)

**Subcellular Localization of tPA.** The possibility that neuronal tPA is compartmentalized to be released as a neuromodulator was next explored. Typically,  $\text{Ca}^{2+}$ -dependent exocytosis of neurotransmitters and neuropeptides requires their compartmentalization into specific secretory organelles [41] classified as synaptic vesicles (SVs) and dense core vesicles (DCVs). To test whether tPA might be stored in synaptic vesicles (SVs), we isolated these organelles from mouse brain extracts using a classical isolation procedure combining subcellular

fractionation and size exclusion chromatography [26]. Immunoblot analysis of the isolated organelles revealed that they contain typical vesicular membrane proteins such as synaptobrevin 2 (Sb2), synaptotagmin 1 (Sy1), synaptophysin 1 (Syp1), the glutamatergic marker vGluT1, the proton pump V-ATPase, and synaptic vesicle 2 (SV2; Fig. 7b). The isolated SVs were virtually free of contamination as evident from the absence of markers for peroxisomes (70-kDa peroxisomal membrane protein, PMP70), recycling endosomes (transferrin receptor,

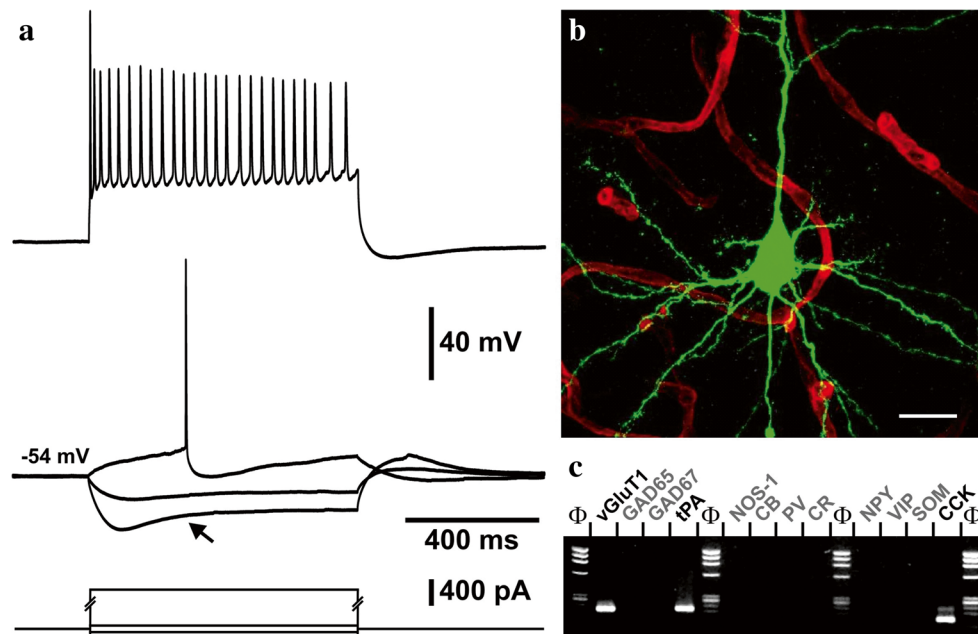


**Fig. 5** Electrophysiological, morphological, and molecular characterization of tPA-expressing layer V pyramidal cell. **a** Voltage responses induced by injection of current pulses (bottom traces) of  $-100$ ,  $-50$ ,  $+20$ , and  $+500$  pA. Note the pronounced voltage sag after the initial peak response to hyperpolarizing current pulses (middle traces, *arrow*). In response to just-above-threshold current pulse ( $+20$  pA), this neuron fired a long-duration action potential with a long-lasting biphasic AHP (middle trace). Near saturation ( $+500$  pA), this neuron showed the typical firing of a regular spiking neuron with marked frequency

adaptation and amplitude accommodation of action potentials (upper trace). **b** Confocal image of the recorded pyramidal cell shown in **(a)** (biocytin labeling; *green*) located in the vicinity of parenchymal capillaries (immunostained for collagen IV; *red*). Note the pyramidal shaped soma with spiny dendrites (*scale bar*  $20\ \mu\text{m}$ ). **c** scRT-mPCR analysis showing expression of tPA, vesicular glutamate transporter 1 (Vglut1), and cholecystokinin (CCK) mRNAs in this pyramidal cell (Color figure online)

TfR), and plasma membrane (the glutamatergic NMDA receptor subunit GluN1 and  $\text{Na}^+/\text{K}^+$ -ATPase). Strikingly, the isolated organelles were negative for chromogranin B (CgB), a specific marker of DCVs (Fig. 7a). Most importantly, the isolated SVs were positive for tPA (Fig. 7b) indicating that tPA is stored in secretory compartment most likely representing subsets of SVs. The vesicular storage of tPA was further confirmed by immunoisolation of Sb2-containing SVs [42, 43] (Fig. 7c, d, f). Such biochemical scenario so far suggests that tPA is co-stored with glutamate in glutamatergic SVs. To further examine whether this is the case, we performed glutamate uptake assays on purified Sb2-positive SVs by acidification measurements using acridine orange [27]. As shown in Fig. 7e, addition of glutamate consistently induced a robust ATP-dependent acidification confirming that our preparation contains a functional population of glutamatergic SVs. The presence of tPA containing SVs was confirmed by confocal immunofluorescence analyses demonstrating a co-localization of Sb2 with tPA in cortical neurons (Fig. 7f).

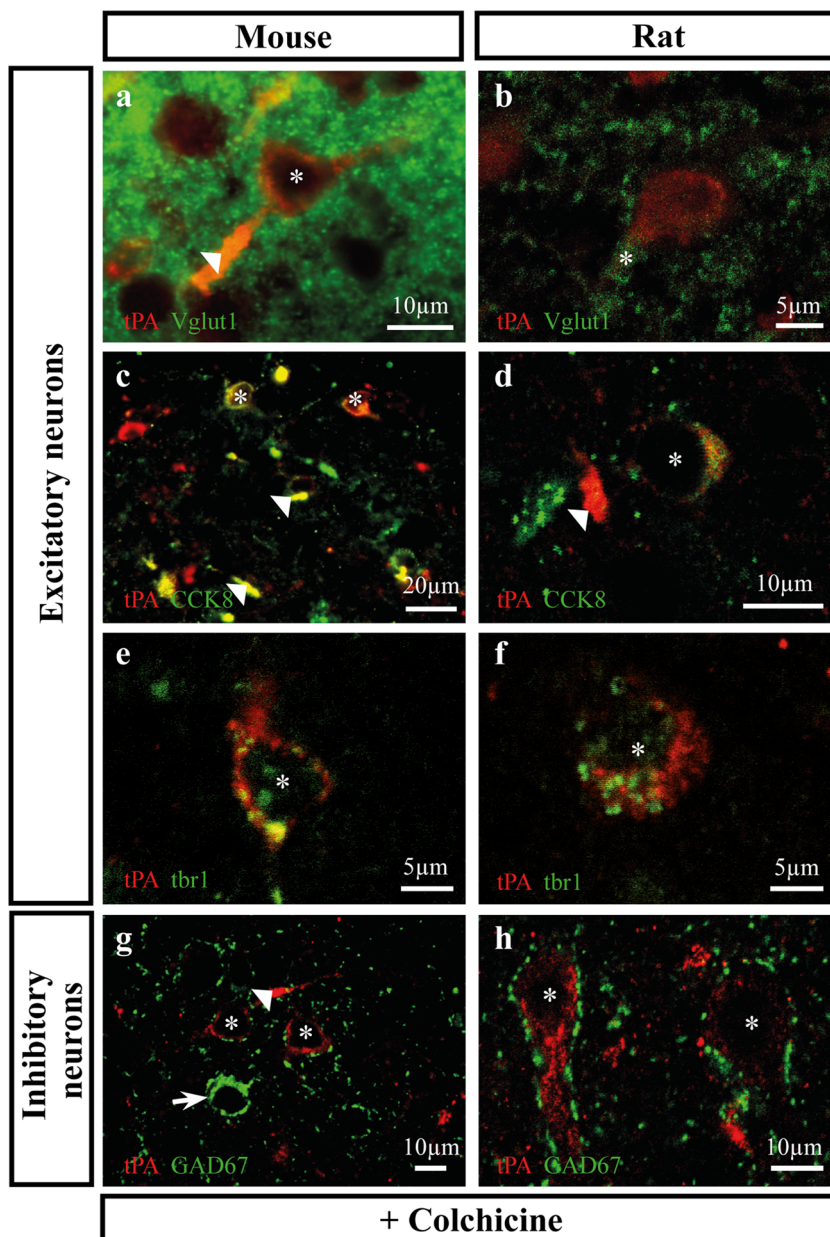
Altogether, our present data provide the first evidence that the tPA is a neuromodulator characteristic of a subpopulation (10–15 %) of pyramidal excitatory glutamatergic neurons with a storage in synaptobrevin-2-positive synaptic vesicles.

## Discussion

tPA plays critical roles in the CNS physiopathology. Surprisingly, uncontroversial information about its regional, cellular, and subcellular distribution is still lacking. To date, endothelial cells forming microvessels are considered as a major source of tPA [44, 45]. Although tPA messenger RNA (mRNA) and tPA proteolytic activity have been detected in astrocytes, this was only reported *in vitro* [46, 47] or following brain injuries [48, 49]. tPA was also found in microglia by some [29, 47] but not all authors [50]. Oligodendrocytes do not display tPA activity *in vitro* [51], but a study showed that they exhibit immunostaining for tPA *in vivo* [20]. Perivascular mastocytes [52], pericytes [53], ependymocytes [54], and infiltrating blood cells [55] are other putative sources of tPA in the CNS. Here, in the adult healthy mouse or rat brain, we found positive immunostainings for tPA in endothelial cells, oligodendrocytes, mastocytes, and ependymocytes, but not in astrocytes, microglia, and pericytes. Focusing on neurons, we detected tPA in neuronal fibers in the hippocampus (mossy fiber pathway), the amygdala, the hypothalamus, and the neurohypophysis as previously reported [56, 57] but also in fibers of the medial habenula. We did not detect tPA in the somata of cortical neurons in normal conditions (neither in rats nor in mice). This was intriguing, considering the documented



**Fig. 6** tPA expression is restricted to cortical glutamatergic neurons in mice and rats. tPA-ir was observed in mice (**a, c, e**) and rats (**b, d, f**) excitatory neurons. Double immunofluorescence stainings were performed using anti-tPA (*red*) and a set of antibodies (*green*) characteristic of excitatory neurons [vGluT1 antibody (**a, b**), cholecystokinin antibody (CCK; **c, d**), and T-box brain 1 antibody (*tbr1*; **e, f**) or inhibitory neurons [GAD 67 (**g, h**)]. In mice and rats, tPA-ir was observed in excitatory vGluT1-positive neurons (**a, b**; *stars*), CCK8-positive neurons (**c, d**; *stars*), and *tbr1*-positive neurons (**e, f**; *stars*). tPA-ir was absent in inhibitory GAD67-positive neurons in mouse (**g**; *arrow*), and in both mouse and rat, GAD67-ir was absent in tPA-positive neurons (**g, f**; *stars*). tPA-positive shrunken fibers were observed (**a, c, d, g**; *arrowheads*) (Color figure online)



presence and actions of endogenous tPA in the cortex [30, 58, 59]. In vitro studies have also reported the neuronal expression of tPA concentrated at the growth cone during neuritogenesis, locally synthesized in dendrites, and released following depolarization [60–64]. Blocking the axo-dendritic transport, using the microtubule uncoupling agent colchicine, allowed to unmask tPA in several hippocampal and cortical neuronal cell bodies (10 to 15 % of cortical neurons). This effect of colchicine was selective of neurons, since the pattern of tPA expression was unchanged in other cell types. This colchicine-induced unmasking of tPA immunoreactivity can be explained either by a rare expression of neuronal tPA or by its fast transport and/or turnover. Anyhow, this approach allowed us to map, for the first time, tPA-positive cortical neurons. In the

mouse hippocampus, tPA was ferreted out in CA1, CA2, and CA3 neuronal cell bodies, in neurons of dentate gyrus, and fasciola cinereum. Although tPA is not present in rat hippocampal mossy fibers [57], tPA-positive neurons appeared in almost all cortical areas in the two species, including the retrosplenial granular, the primary somatosensory, and the perirhinal and the piriform cortices. Neuronal tPA is also present in other structures such as the amygdala, the bed nucleus of the stria terminalis, or the cingulum.

Our data are in agreement with the reported physiopathological functions of tPA in the CNS. For example, tPA was reported to be critically involved in spatial learning and memory processes known to involve both the hippocampus and the entorhinal cortex, in anxiety behavior known to involve the

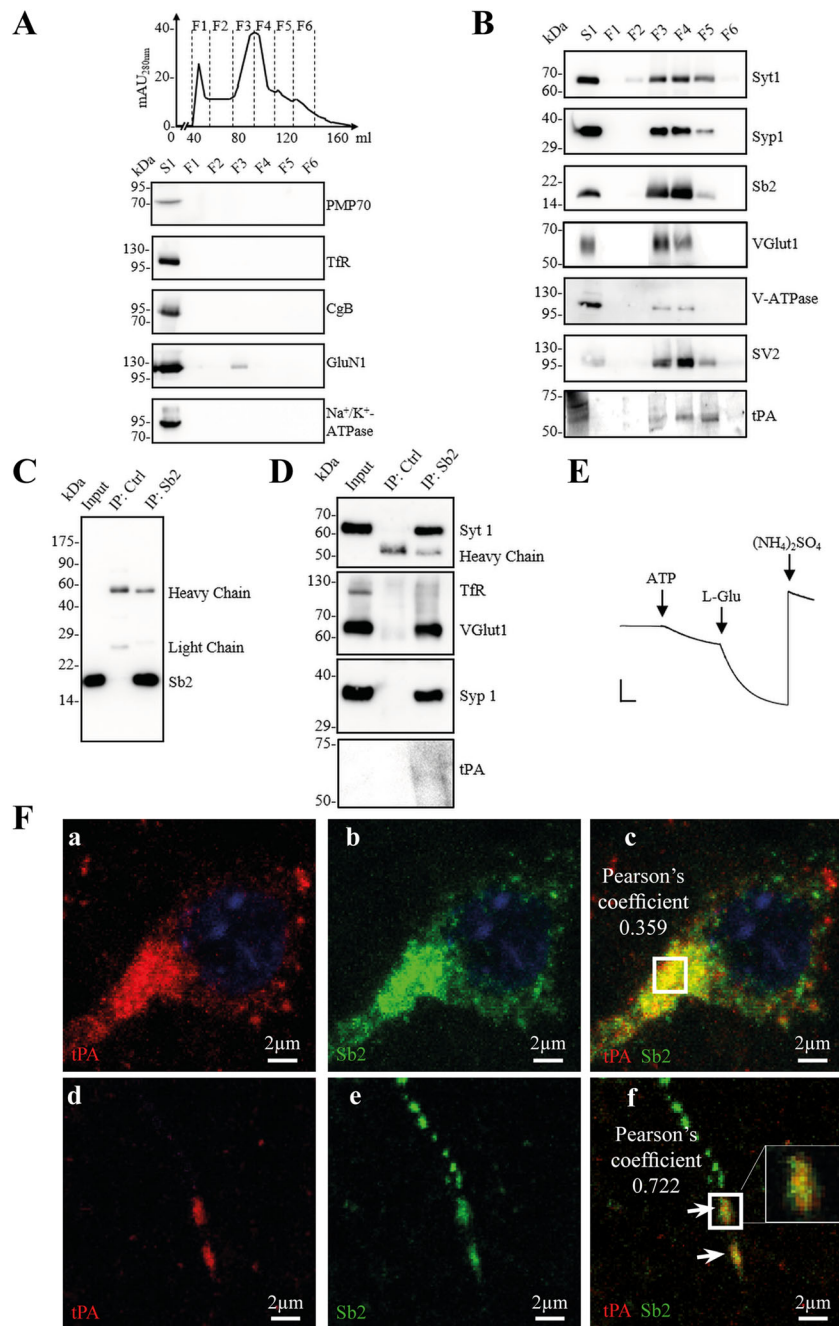


**Fig. 7** tPA is localized in Sv2-containing SVs. **a** Isolation of SVs by size exclusion chromatography led to six fractions (F1–F6). The brain supernatant S1 and F1–F6 were immunoblotted for the markers of peroxisomes (70-kDa peroxisomal membrane protein, PMP70), recycling endosomes (transferrin receptor, TfR), dense core vesicles (chromogranin B, CgB), and plasma membrane (the NMDA receptor subunit GluN1 and  $\text{Na}^+/\text{K}^+$ -ATPase). GluN1 is detected at a low level in F3, suggesting that proteins from the plasma membrane use SVs as recycling vesicles. **b** The isolated organelles contain the typical SV markers synaptotagmin I (Syt1), synaptophysin 1 (Syp1), Sv2, vGlut1, and V-ATPase. SVs are mostly present in F3 and F4, and in a lower level in F5. S1 and F1–F6 were also immunoblotted for tPA. **c** Immunoprecipitation of SVs was performed using Sv2 and a non-immune IgG as control. Note the presence in the immunisolates of the

light and heavy chains of the antibodies used for the SV isolation. **d** Immunoblots showed that immunoprecipitated SVs presented typical SV markers. Brain supernatant (input) and immunoprecipitates (IP) were immunoblotted for tPA (goat anti-tPA). Equal proportion of F1–F6 and of IPs were loaded to allow direct comparison. **e** Photometric traces (typical experiment) for immunoprecipitated SVs showing their acidification induced by glutamate (10 mM). At the end of the reaction,  $(\text{NH}_4)_2\text{SO}_4$  (100 mM) was added to dissipate the pH gradient. Scale bar, 5 arbitrary units per 100 s. **f** Double immunofluorescent stainings revealed with rabbit anti-tPA antibodies (*a, c, d, f; red*) and mouse anti-Sv2 antibodies (*b, c, e, f; green*). tPA-ir was closely associated with Sv2-ir in cortical neuronal cell bodies (*c; yellow*) and corresponding fiber tracks (*f; yellow*). Colocalization of tPA-ir and Sv2-ir was confirmed by Pearson's coefficient, 0.359 (*c*) and 0.722 (*f*) (Color figure online)

amygdala and in a number of sensorimotor tasks [4, 5, 65–67]. Under pathological conditions, tPA was reported to play critical roles in delayed hippocampal neuronal death following kainate exposure, in seizure, and in survival and death of cortical neurons [15, 29, 68, 69].

In order to characterize the phenotype of tPA-ergic neurons, single neurons of the rat somatosensory cortex were patched and subjected to combined electrophysiological and transcriptomic analyses. We found that neurons containing tPA mRNA display the electrophysiological, morphological, and molecular features of excitatory pyramidal glutamatergic neurons. Indeed, tPA-positive pyramidal neurons characteristically exhibit regular spiking action potential discharge [34], including long-duration action potentials and pronounced spike frequency adaptation. Biocytin labeling of recorded neurons revealed that tPA-positive neurons are pyramidal spiny neurons and none of the tPA-positive neurons expressed exclusive markers of GABA-ergic interneurons. Immunohistochemical analyses confirmed the presence of vGlut1, CCK8, and the transcription factor *tbR1* in tPA-positive neurons.

Our finding that tPA-ergic neurons are excitatory is consistent with the reported functional link between tPA and NMDA-receptor-dependent glutamatergic signaling [17] involved in long-term potentiation [3, 70], synaptic plasticity [71], seizure [68], neuronal death [72], and survival [6]. Of note, tPA-positive neurons receive projections from GABA-ergic neurons. In vitro, neuronal depolarization induced by GABA receptor antagonists such as bicuculline leads to a massive release of neuronal tPA [73]. Isolation of SVs by subcellular fractionation followed by size exclusion chromatography confirmed the presence of tPA in neuronal vesicles. SVs isolated by this method are clear and small vesicles as previously described [26]. Also, tPA is more detected in F4 and F5 suggesting its presence in more retarded vesicles, i.e., smaller than the main population of SVs. Immunoprecipitations performed with an antibody against Sb2 but also co-immunostaining of tPA and Sb2 confirmed the presence of tPA in Sb2-positive neuronal vesicles. The presence of overexpressed tPA in organelles, which seem to be DCVs, was previously reported by Silverman and colleagues [74]. Although we failed to detect CgB in the isolated fractions, it is known that subsets of DCVs are positive for Sb2 [75]. Our data are relevant with the literature that evidences the presence of tPA in synaptic spines [62, 63], its possible constitutive neuronal release [64], and also its early and massive release from synapses following KCl- [63] or bicuculline-induced depolarization [73]. This observation is also relevant with the neuromodulatory functions of tPA, especially its ability to bind postsynaptic NMDA receptors and promote their signaling [76] including the late phase of long-term potentiation [77] and excitotoxicity [72].

Altogether, we provide here a set of compelling histological, electrophysiological, and transcriptional evidence

demonstrating the existence of a population of excitatory glutamatergic pyramidal neurons with tPA-containing synaptobrevin-2-positive synaptic vesicles that allow us to propose the concept of tPA-ergic neurons.

**Acknowledgments** This work was supported by grants from the INSERM (French National Institute for Health and Medical Research) (D.V.), the University of Caen Basse-Normandie (D.V.), Era-net Neuron program “ProteA” EU FP7 (D.V.), ANR 2011 MALZ 003 01 (B.C.), and “IHU Institut de Neurosciences Translationnelles de Paris,” ANR-10-IAIHU-06 (B.C. and B.L.). Part of this work was coordinated by CEA/MIRCen/IB2M and supported by the association France Alzheimer (B.C.). G.M. is supported by a grant from the Fondation pour la Recherche Médicale and J-P.M. receives operating grants from Centre National de la Recherche Scientifique, France Alzheimer, and Université Aix-Marseille. The authors also thanks Pr.Carine ALI for her suggestions during the elaboration of the manuscript.

## References

1. Astrup T, Stage A (1952) Isolation of a soluble fibrinolytic activator from animal tissue. *Nature* 170:929
2. Tanswell P, Seifried E, Su PC et al (1989) Pharmacokinetics and systemic effects of tissue-type plasminogen activator in normal subjects. *Clin Pharmacol Ther* 46:155–62
3. Baranes D, Lederfein D, Huang Y, Chen M (1998) Tissue plasminogen activator contributes to the late phase of LTP and to synaptic growth in the hippocampal mossy fiber pathway. *Neuron* 21:813–825
4. Madani R, Hulo S, Toni N et al (1999) Enhanced hippocampal long-term potentiation and learning by increased neuronal expression of tissue-type plasminogen activator in transgenic mice. *EMBO J* 18:3007–12. doi:10.1093/emboj/18.11.3007
5. Pawlak R, Magarinos AM, Melchor J et al (2003) Tissue plasminogen activator in the amygdala is critical for stress-induced anxiety-like behavior. *Nat Neurosci* 6:168–174. doi:10.1038/nn998
6. Yepes M, Lawrence DA (2004) Tissue-type plasminogen activator and neuroserpin: a well-balanced act in the nervous system? *Trends Cardiovasc Med* 14:173–80. doi:10.1016/j.tcm.2004.03.004
7. Jacobsen JS, Comery TA, Martone RL et al (2008) Enhanced clearance of Aβeta in brain by sustaining the plasmin proteolysis cascade. *Proc Natl Acad Sci U S A* 105:8754–9. doi:10.1073/pnas.0710823105
8. Bukhari N, Torres L, Robinson JK, Tsirka SE (2011) Axonal regrowth after spinal cord injury via chondroitinase and the tissue plasminogen activator (tPA)/plasmin system. *J Neurosci* 31:14931–43. doi:10.1523/JNEUROSCI.3339-11.2011
9. Obiang P, Macrez R, Jullienne A et al (2012) GluN2D subunit-containing NMDA receptors control tissue plasminogen activator-mediated spatial memory. *J Neurosci* 32:12726–34. doi:10.1523/JNEUROSCI.6202-11.2012
10. Yepes M, Roussel BD, Ali C, Vivien D (2009) Tissue-type plasminogen activator in the ischemic brain: more than a thrombolytic. *Trends Neurosci* 32:48–55. doi:10.1016/j.tins.2008.09.006
11. García-Rocha M, Avila J, Armas-Portela R (1994) Tissue-type plasminogen activator (tPA) is the main plasminogen activator associated with isolated rat nerve growth cones. *Neurosci Lett* 180:123–126. doi:10.1016/0304-3940(94)90502-9
12. Bruno MA, Cuello AC (2006) Activity-dependent release of precursor nerve growth factor, conversion to mature nerve growth factor, and its degradation by a protease cascade. *Proc Natl Acad Sci U S A* 103:6735–40. doi:10.1073/pnas.0510645103

13. Rodier M, Prigent-Tessier A, Béjot Y et al (2014) Exogenous t-PA Administration Increases Hippocampal Mature BDNF Levels. Plasmin- or NMDA-Dependent Mechanism? *PLoS One* 9: e92416. doi:10.1371/journal.pone.0092416
14. Orth K, Willnow T, Herz J et al (1994) Low density lipoprotein receptor-related protein is necessary for the internalization of both tissue-type plasminogen activator-inhibitor complexes and free tissue-type plasminogen activator. *J Biol Chem* 269:21117–22
15. Yepes M, Sandkvist M, Moore EG et al (2003) Tissue-type plasminogen activator induces opening of the blood–brain barrier via the LDL receptor-related protein. *J Clin Invest* 112:1533–1540. doi:10.1172/JCI200319212.Introduction
16. Benchenane K, Berezowski V, Ali C et al (2005) Tissue-type plasminogen activator crosses the intact blood–brain barrier by low-density lipoprotein receptor-related protein-mediated transcytosis. *Circulation* 111:2241–9. doi:10.1161/01.CIR.0000163542.48611.A2
17. Nicole O, Docagne F, Ali C et al (2001) The proteolytic activity of tissue-plasminogen activator enhances NMDA receptor-mediated signaling. *Nat Med* 7:59–64. doi:10.1038/83358
18. Samson AL, Nevin ST, Croucher D et al (2008) Tissue-type plasminogen activator requires a co-receptor to enhance NMDA receptor function. *J Neurochem* 107:1091–101. doi:10.1111/j.1471-4159.2008.05687.x
19. Siao C-J, Tsirka SE (2002) Tissue plasminogen activator mediates microglial activation via its finger domain through annexin II. *J Neurosci* 22:3352–8. doi:10.1523/JNEUROSCI.0058-09.2009
20. Correa F, Gauberti M, Parcq J et al (2011) Tissue plasminogen activator prevents white matter damage following stroke. *J Exp Med* 208:1229–42. doi:10.1084/jem.20101880
21. Mascagni F, McDonald AJ (2003) Immunohistochemical characterization of cholecystokinin containing neurons in the rat basolateral amygdala. *Brain Res* 976:171–184. doi:10.1016/S0006-8993(03)02625-8
22. Stanić D, Mulder J, Watanabe M, Hökfelt T (2011) Characterization of NPY Y2 receptor protein expression in the mouse brain. II. Coexistence with NPY, the Y1 receptor, and other neurotransmitter-related molecules. *J Comp Neurol* 519:1219–57. doi:10.1002/cne.22608
23. Karagiannis A, Gallopin T, Dávid C et al (2009) Classification of NPY-expressing neocortical interneurons. *J Neurosci* 29:3642–59. doi:10.1523/JNEUROSCI.0058-09.2009
24. Cauli B, Audinat E, Lambolez B et al (1997) Molecular and physiological diversity of cortical nonpyramidal cells. *J Neurosci* 17:3894–906
25. Lambolez B, Audinat E, Bochet P et al (1992) AMPA receptor subunits expressed by single purkinje cells. *Neuron* 9:247–258. doi:10.1016/0896-6273(92)90164-9
26. Ahmed S, Holt M, Riedel D, Jahn R (2013) Small-scale isolation of synaptic vesicles from mammalian brain. *Nat Protoc* 8:998–1009. doi:10.1038/nprot.2013.053
27. Martineau M, Shi T, Puyal J et al (2013) Storage and uptake of D-serine into astrocytic synaptic-like vesicles specify gliotransmission. *J Neurosci* 33:3413–23. doi:10.1523/JNEUROSCI.3497-12.2013
28. Gualandris A, Jones TE, Strickland S, Tsirka SE (1996) Membrane Depolarization Induces Calcium-Dependent Secretion of Tissue Plasminogen activator. *J Neurosci* 16:2220–2225
29. Tsirka S, Rogove A, Bugge T et al (1997) An extracellular proteolytic cascade promotes neuronal degeneration in the mouse hippocampus. *J Neurosci* 17:543–552
30. Teesalu T, Kulla A, Simisker A (2004) Tissue plasminogen activator and neuroserpin are widely expressed in the human central nervous system. *Thromb Haemost* 92:358–368. doi:10.1160/TH02-12-0310
31. Castorina A, D’Amico AG, Scuderi S et al (2013) Dopamine D3 receptor deletion increases tissue plasminogen activator (tPA) activity in prefrontal cortex and hippocampus. *Neuroscience* 250:546–56. doi:10.1016/j.neuroscience.2013.07.053
32. Li J, Yu L, Gu X, et al. (2013) Tissue plasminogen activator regulates Purkinje neuron development and survival. *Proc Natl Acad Sci U S A* 1–10. doi:10.1073/pnas.1305010110
33. Ascoli GA, Alonso-Nanclares L, Anderson SA et al (2008) Petilla terminology: nomenclature of features of GABAergic interneurons of the cerebral cortex. *Nat Rev Neurosci* 9:557–68. doi:10.1038/nrn2402
34. McCormick DA, Connors BW, Lighthall JW, Prince DA (1985) Comparative electrophysiology of pyramidal and sparsely spiny stellate neurons of the neocortex. *J Neurophysiol* 54:782–806
35. Connors BW, Gutnick MJ (1990) Intrinsic firing patterns of diverse neocortical neurons. *Trends Neurosci* 13:99–104
36. Kasper EM, Lübke J, Larkman AU, Blakemore C (1994) Pyramidal neurons in layer 5 of the rat visual cortex. III. Differential maturation of axon targeting, dendritic morphology, and electrophysiological properties. *J Comp Neurol* 339:495–518. doi:10.1002/cne.903390404
37. Christophe E, Doerflinger N, Lavery DJ et al (2005) Two populations of layer v pyramidal cells of the mouse neocortex: development and sensitivity to anesthetics. *J Neurophysiol* 94:3357–67. doi:10.1152/jn.00076.2005
38. Voelker CCJ, Garin N, Taylor JSH et al (2004) Selective neurofilament (SMI-32, FNP-7 and N200) expression in subpopulations of layer v pyramidal neurons in vivo and in vitro. *Cereb Cortex* 14:1276–86. doi:10.1093/cercor/bhh089
39. Sorensen SA, Bernard A, Menon V et al (2015) Correlated gene expression and target specificity demonstrate excitatory projection neuron diversity. *Cereb Cortex* 25:433–49. doi:10.1093/cercor/bht243
40. Hevner RF, Shi L, Justice N et al (2001) Tbr1 Regulates Differentiation of the Preplate and Layer 6. *Neuron* 29:353–366. doi:10.1016/S0896-6273(01)00211-2
41. Jahn R, Fasshauer D (2012) Molecular machines governing exocytosis of synaptic vesicles. *Nature* 490:201–7. doi:10.1038/nature11320
42. Crippa D, Schenk U, Francolini M et al (2006) Synaptobrevin2-expressing vesicles in rat astrocytes: insights into molecular characterization, dynamics and exocytosis. *J Physiol* 570:567–82. doi:10.1113/jphysiol.2005.094052
43. Martineau M, Galli T, Baux G, Mothet J-P (2008) Confocal imaging and tracking of the exocytotic routes for D-serine-mediated gliotransmission. *Glia* 56:1271–84. doi:10.1002/glia.20696
44. Zlokovic BV, Wang L, Sun N et al (1995) Expression of tissue plasminogen activator in cerebral capillaries: possible fibrinolytic function of the blood–brain barrier. *Neurosurgery* 37:955–961
45. Levin EG, Santell L, Osborn KG (1997) The expression of endothelial tissue plasminogen activator in vivo: a function defined by vessel size and anatomic location. *J Cell Sci* 110:139–48
46. Docagne F, Nicole O, Marti HH et al (1999) Transforming growth factor-beta1 as a regulator of the serpins/t-PA axis in cerebral ischemia. *FASEB J* 13:1315–24
47. Joo SH, Kwon KJ, Kim JW et al (2010) Regulation of matrix metalloproteinase-9 and tissue plasminogen activator activity by alpha-synuclein in rat primary glial cells. *Neurosci Lett* 469:352–6. doi:10.1016/j.neulet.2009.12.026
48. Adhami F, Yu D, Yin W et al (2008) Deleterious effects of plasminogen activators in neonatal cerebral hypoxia-ischemia. *Am J Pathol* 172:1704–16. doi:10.2353/ajpath.2008.070979
49. Kim JW, Lee SH, Ko HM et al (2011) Biphasic regulation of tissue plasminogen activator activity in ischemic rat brain and in cultured neural cells: essential role of astrocyte-derived plasminogen

- activator inhibitor-1. *Neurochem Int* 58:423–33. doi:[10.1016/j.neuint.2010.12.020](https://doi.org/10.1016/j.neuint.2010.12.020)
50. Ludwig R, Feindt J, Lucius R et al (1996) Metabolism of neuro-peptide Y and calcitonin gene-related peptide by cultivated neurons and glial cells. *Brain Res Mol Brain Res* 37:181–91
  51. Kalderon N, Ahonen K, Fedoroff S (1990) Developmental transition in plasticity properties of differentiating astrocytes: age-related biochemical profile of plasminogen activators in astroglial cultures. *Glia* 3:413–26. doi:[10.1002/glia.440030513](https://doi.org/10.1002/glia.440030513)
  52. Sillaber C, Baghestanian M, Bevec D et al (1999) The mast cell as site of tissue-type plasminogen activator expression and fibrinolysis. *J Immunol* 162:1032–41
  53. Yamamoto C, Sugato M, Fujiwara Y, Kaji T (2005) Selective promotion of plasminogen activator inhibitor-1 secretion by activation of proteinase-activated receptor-1 in cultured human brain microvascular pericytes: comparison with endothelial cells. *Biol Pharm Bull* 28:208–11
  54. Ware J, Dibenedetto A, Pittman R (1995) Localization of tissue plasminogen activator mRNA in adult rat brain. *Brain Res Bull* 37:275–281
  55. Tabengwa EM, Wheeler CG, Yancey DA et al (2002) Alcohol-Induced Up-Regulation of Fibrinolytic Activity and Plasminogen Activators in Human Monocytes. *Alcohol Clin Exp Res* 26:1121–1127. doi:[10.1111/j.1530-0277.2002.tb02647.x](https://doi.org/10.1111/j.1530-0277.2002.tb02647.x)
  56. Sappino A, Madani R, Huarte J (1993) Extracellular proteolysis in the adult murine brain. *J Clin Invest* 92:679–685
  57. Salles FJ, Strickland S (2002) Localization and regulation of the tissue plasminogen activator-plasmin system in the hippocampus. *J Neurosci* 22:2125–34
  58. Seeds NW, Williams BL, Bickford PC (1995) Tissue Plasminogen Activator Induction in Purkinje Neurons After Cerebellar Motor Learning. *Science* (80- ) 270:1992–1994.
  59. Cho M-K, Sun E-S, Kim Y-H (2013) Zinc-triggered induction of tissue plasminogen activator and plasminogen in endothelial cells and pericytes. *Exp Neurobiol* 22:315–21. doi:[10.5607/en.2013.22.4.315](https://doi.org/10.5607/en.2013.22.4.315)
  60. Krystosek A, Seeds N (1981) Plasminogen activator release at the neuronal growth cone. *Science* (80- ) 213:1532–1534.
  61. Pittman RN, Ivins JK, Buettner HM (1989) Neuronal plasminogen activators: cell surface binding sites and involvement in neurite outgrowth. *J Neurosci* 9:4269–86
  62. Lochner JE, Kingma M, Kuhn S et al (1998) Real-time imaging of the axonal transport of granules containing a tissue plasminogen activator/green fluorescent protein hybrid. *Mol Biol Cell* 9:2463–76
  63. Lochner JE, Spangler E, Chavarha M et al (2008) Efficient copackaging and cotransport yields postsynaptic colocalization of neuromodulators associated with synaptic plasticity. *Dev Neurobiol* 68:1243–56. doi:[10.1002/dneu.20650](https://doi.org/10.1002/dneu.20650)
  64. Shin CY, Kundel M, Wells DG (2004) Rapid, activity-induced increase in tissue plasminogen activator is mediated by metabotropic glutamate receptor-dependent mRNA translation. *J Neurosci* 24:9425–33. doi:[10.1523/JNEUROSCI.2457-04.2004](https://doi.org/10.1523/JNEUROSCI.2457-04.2004)
  65. Seeds N, Williams B, Bickford P (1995) Tissue plasminogen activator induction in Purkinje neurons after cerebellar motor learning. *Science* (80- ) 270:1992–1994.
  66. Benuer S, Shankaranarayana Rao BS, Pawlak R et al (2007) Stress-induced spine loss in the medial amygdala is mediated by tissue-plasminogen activator. *Neuroscience* 144:8–16. doi:[10.1016/j.neuroscience.2006.08.075](https://doi.org/10.1016/j.neuroscience.2006.08.075)
  67. Gorter JA, Van Vliet EA, Rauwerda H et al (2007) Dynamic changes of proteases and protease inhibitors revealed by microarray analysis in CA3 and entorhinal cortex during epileptogenesis in the rat. *Epilepsia* 48:53–64. doi:[10.1111/j.1528-1167.2007.01290.x](https://doi.org/10.1111/j.1528-1167.2007.01290.x)
  68. Tsirka S, Gualandris A, Amaral D, Strickland S (1995) Excitotoxin-induced neuronal degeneration and seizure are mediated by tissue plasminogen activator. *Nature* 377:340–344
  69. Siao C-J, Fernandez SR, Tsirka SE (2003) Cell type-specific roles for tissue plasminogen activator released by neurons or microglia after excitotoxic injury. *J Neurosci* 23:3234–42
  70. Pang PT, Teng HK, Zaitsev E et al (2004) Cleavage of proBDNF by tPA/plasmin is essential for long-term hippocampal plasticity. *Science* 306:487–91. doi:[10.1126/science.1100135](https://doi.org/10.1126/science.1100135)
  71. Samson AL, Medcalf RL (2006) Tissue-type plasminogen activator: minireview a multifaceted modulator of neurotransmission and synaptic plasticity. *Neuron* 50:673–678. doi:[10.1016/j.neuron.2006.04.013](https://doi.org/10.1016/j.neuron.2006.04.013)
  72. Baron A, Montagne A, Cassé F et al (2010) NR2D-containing NMDA receptors mediate tissue plasminogen activator-promoted neuronal excitotoxicity. *Cell Death Differ* 17:860–71. doi:[10.1038/cdd.2009.172](https://doi.org/10.1038/cdd.2009.172)
  73. Centonze D, Napolitano M, Saulle E et al (2002) Tissue plasminogen activator is required for corticostriatal long-term potentiation. *Eur J Neurosci* 16:713–721. doi:[10.1046/j.1460-9568.2002.02106.x](https://doi.org/10.1046/j.1460-9568.2002.02106.x)
  74. Silverman MA, Johnson S, Gurkins D et al (2005) Mechanisms of transport and exocytosis of dense-core granules containing tissue plasminogen activator in developing hippocampal neurons. *J Neurosci* 25:3095–106. doi:[10.1523/JNEUROSCI.4694-04.2005](https://doi.org/10.1523/JNEUROSCI.4694-04.2005)
  75. Tobin V, Schwab Y, Lelos N et al (2012) Expression of exocytosis proteins in rat supraoptic nucleus neurones. *J Neuroendocrinol* 24:629–41. doi:[10.1111/j.1365-2826.2011.02237.x](https://doi.org/10.1111/j.1365-2826.2011.02237.x)
  76. Fernández-Monreal M, López-Atalaya JP, Benchenane K et al (2004) Arginine 260 of the amino-terminal domain of NR1 subunit is critical for tissue-type plasminogen activator-mediated enhancement of N-methyl-D-aspartate receptor signaling. *J Biol Chem* 279:50850–6. doi:[10.1074/jbc.M407069200](https://doi.org/10.1074/jbc.M407069200)
  77. Zhuo M, Holtzman DM, Li Y et al (2000) Role of tissue plasminogen activator receptor LRP in hippocampal long-term potentiation. *J Neurosci* 20:542–9